32nd Congress of the International Council of the Aeronautical Sciences
September 6-10, 2021
Pudong Shangri-La, Shanghai, China

SYNERGETIC CONTROLS OF THE SYSTEM "CARRIER AIRCRAFT - UPPER-STAGE ROCKET"

Kreerenko Olga

Moscow Aviation Institute
Beriev Aircraft Company

Abstract

In current times, one of the priority tasks of modern cosmonautics is to increasing payload mass putting into orbit. The best choice for this purpose, is aerospace systems (AS), which consisting of carrier aircraft (CA) and upper-stage rocket (USR), located on its upper surface. They can carry out an air launch near the equator. Feature of such complexes is the organization of automatic control modes. There is a tendency to expand the range of tasks, solved by onboard automatic control systems. Requirements for their reliability and efficiency are becoming tougher. In this regard, the problem of designing a new class of autopilot acquires obvious relevance. The article proposes a new approach to design control strategies for system "carrier aircraft - upper-stage rocket", based on principals and methods of synergetic control theory. Proposed approach allows performing control strategies for the system "carrier aircraft - upper-stage rocket", ensuring asymptotic stability of closed system in entire permissible range of phase coordinates and system invariance to external disturbances. Synthesis of the controller is performed with using full nonlinear model of motion of flight vehicle with account for aerodynamic and force interaction between flight vehicles (FV). Researching of dynamic properties of closed nonlinear system was produced with computer simulation with using parameters of specific aircraft. Exact fulfillment of predetermined technological invariants is demonstrated.

Keywords: synergetic control, carrier aircraft, invariant, flight vehicle.

1. Introduction

In order to increase the fuel efficiency and payload of space systems, at the present stage of space exploration, scientists and engineers are increasingly inclined to use multistage aerospace systems for launching spacecraft into orbit, with upper-stage rocket, located on a carrier aircrafts upper surface. Taking into account the summary world statistics on the number of emergency space launches from ground-based cosmodromes (from 1957 to 2014: Russia - 5%; China - 5.1%; Europe - 6.6%; USA - 8.3%; platforms of the Sea start "–8.3%) the task of increasing the efficiency, safety and accuracy of the functioning of such aerospace complexes (with the upper location of the detachable aircraft on the carrier aircraft) at the stage of taking to the air launch site, as well as when separating the stages, is very urgent. Due to the mobility of the second stage air launch point, errors in position in space and time of aircraft separation may occur. With the upper position of the USR, the solution of the problem of separating the aircraft presents certain difficulties. With the upper location of the upper stage, the solution of the problem of separating the aircraft presents certain difficulties: it is necessary to ensure the safe mutual movement of the separated aircraft after the moment of breaking the mechanical bonds. A number of foreign studies have been devoted to solving these and other similar problems, starting from the 60s of the XX century, the results of which were published in the works of scientists and engineers at the NASA Research Center, Langley; Center for Analytical Mechanics in Hampton? (USA); Munich Technical University;

German Aerospace Center, Institute for Dynamic Systems and Control (Germany) [1-6]. In the Soviet Union, these problems discussed during the development of a system for separating the Buran reusable aerospace aircraft from the launch vehicle. Theoretical and applied research to determine the features of the aircraft separation process was carried out by specialists from the Central Aerohydrodynamic Institute (TsAGI) [7-10].

The process of separating of flight vehicles is a technically complex and dangerous procedure. It is necessary to exclude the collision of aircraft, the negative impact on the structure of the aircraft carrier of the jet of heated gases from the engines of the upper stage; to minimize errors in piloting, to ensure the invariance of the system to the effects of various kinds of disturbances. The solution to these problems is possible with the help of ASS flight control systems at the most critical stages.

Modern methods of developing control laws for autopilots and automatic flight control systems originate from the works of A.M. Letov (solving the problem of analytical design of controllers) [11], developed in the works of Academician A.A. Krasovsky and his followers (methods using generalized work functional) [12]. V.N. Bukov applied methods based on the functional of generalized work for the analytical construction of optimal control laws using predictive models. He also developed adaptive control algorithms that combine the synthesis of control and the estimation of the parameters of the controlled process in real time [13]. Nonlinear and adaptive control of spatial motion of complex dynamic systems is presented in the works of V.O. Nikiforova, I.V. Miroshnik, A.L. Fradkov [14]. A great contribution to the solution of applied problems of the development of stabilization systems for spacecraft carriers was made by Ya.E. Eisenberg [15].

The aerospace complex considered in this study is a two-stage system. The first stage is an amphibious aircraft (carrier aircraft); the second stage is a hypersonic aircraft (upper stage) located on top of the carrier aircraft. The carrier aircraft and the upper stage included in the ASS are complex nonlinear control objects (CO). The dynamics of motion of such objects is described by a system of nonlinear differential equations. The task of controlling the entire complex as a whole at the stage of joint flight, as well as the carrier aircraft and the upper stage during their separation and autonomous flight is multidimensional. The general model of the aerospace systems behavior is supplemented by nonlinear components of the dynamics of the aircrafts included in it. The force (reactions in communication nodes) and aerodynamic (interference effect) interactions between them are taken into account. The use of existing methods for solving control problems in such a nonlinear setting usually presents certain difficulties associated with the need to linearize mathematical models, the impossibility of solving the Riccati equation for nonlinear objects, etc. To overcome these difficulties, it is proposed to use the approaches of synergetic control theory (SCT). For the synthesis of control systems for the aerospace complex during launch at a given speed to the desired altitude (for air launch); and also to stabilize the speed and altitude of the upper stage and the carrier aircraft after their separation, in this work, it is proposed to use one of the STU methods - the method of analytical design of aggregated regulators (ADAR). ADAR method was developed by Professor A.A. Kolesnikov and developed in the works of his apprentices and followers [16-18]. This method makes it possible to work with a complete nonlinear model of the motion of an aircraft and to carry out coordinated control over all phase variables to transfer the control object to a given state.

1.1 Research objectives

The work considered and solved the following tasks:

– formation of a mathematical model of the dynamics of the longitudinal motion of the CA and USR and a mathematical model of forces in the nodes of communication between them;
– development of a procedure for synergetic synthesis of control algorithms for the rise of the ASS at a given speed to a given height for an air launch of the upper stage;
– development of a procedure for synergistic synthesis of control algorithms for the separation of the upper stage and the carrier aircraft while simultaneously breaking the links between them.

2. Synergetic synthesis of control algorithms for ASS during ascent to a height for air launch of USR

2.1 Mathematical model of the control object

2.1.1 Mathematical model of the longitudinal motion of the ASS

To synthesize the autopilot control law of the aerospace complex at the stage of ascent to a given altitude, we will use the mathematical model of the longitudinal motion of the aircraft in projections on the axis of a semi-connected coordinate system [13]. Let us supplement it with the projections of the forces $N_x^{псв}$, $N_y^{псв}$, and the moment M_{zN} in the communication nodes between the CA and USR:

$$
\begin{aligned}
&m\dot{V}(t) = P\cos\alpha - mg\sin(\vartheta-\alpha) - X^{псв} + N_x^{псв};\\
&\dot{H}(t) = V\cdot\sin(\vartheta-\alpha);\\
&mV\dot{\alpha}(t) = mV\omega_z - P\sin\alpha + mg\cos(\vartheta-\alpha) - Y^{псв} + N_y^{псв};\\
&\dot{\omega}_z(t) = \frac{1}{I_z}(M_{za}+M_{zN});\\
&\dot{\vartheta}(t) = \omega_z;\\
&\dot{x}(t) = V\cos(\vartheta-\alpha),
\end{aligned}
\tag{1}
$$

where V – airspeed; H – flight altitude; α – attack angle; ω_z – the angular velocity of the pitch; ϑ – pitch angle; x – longitudinal displacement of the center of gravity (c.g.) of the aircraft;. m – aircraft weight; I_z – the moment of inertia of the aircraft relative to the OZ axis; g – acceleration of gravity; P – engine thrust; $X^{псв}, Y^{псв}$ – drag force and aerodynamic lift force of the aircraft in a semi-connected coordinate system; M_{za} – aerodynamic pitch moment.

$$
\begin{aligned}
X^{псв} &= c_x qS;\\
Y^{псв} &= c_y qS;\\
M_{za} &= m_z qSb_A,
\end{aligned}
\tag{2}
$$

where c_x, c_y, m_z – dimensionless coefficients of drag force, lift force and pitch moment, S – aircraft wing area, l – wingspan; b_A – middle aerodynamic wing chord, q – velocity head:

$$
q = \frac{\rho|V|^2}{2},
\tag{3}
$$

ρ – air density (found according to tables of standard atmosphere depending on altitude) [19].

Taking into account the peculiarities of the AS layout scheme, the expressions for the coefficients of aerodynamic forces and the pitching moment will take the form:

$$
\begin{aligned}
c_x &= c_x(\alpha) + c_x^{\delta_в}\delta_в + k_{in1}\Delta c_{xin};\\
c_y &= c_y(\alpha) + c_y^{\delta_в}\delta_в + k_{in2}\Delta c_{yin};\\
m_z &= m_z(\alpha) + m_z^{\bar{\omega}_z}\bar{\omega}_z + m_z^{\delta_в}\delta_в + k_{in3}\Delta m_{zin},
\end{aligned}
\tag{4}
$$

where $\delta_в$ – elevator deflection angle; $c_x^{\delta_в}$, $c_y^{\delta_в}$, $m_z^{\delta_в}$ – derivatives of the coefficients of the drag force, lift force and pitching moment with respect to $\delta_в$; $\Delta c_{xin}, \Delta c_{yin}, \Delta m_{zin}$ – additions of the coefficients of the drag force, lift and pitching moment from the interference between the CA and USR; $k_{in1}, k_{in2}, k_{in3}$ – coefficients that take into account the change in interference depending on the distance between the CA and USR; $m_z^{\bar{\omega}_z}$ – derivative of the longitudinal moment coefficient with respect to the relative angular pitch velocity $\bar{\omega}_z$ [20].

2.1.2 Determination of forces in communication nodes between ASR and CA

Let us consider a three-support scheme for attaching the upper stage to the carrier aircraft, in which one support is located in front of the center of gravity of the CA and two supports are located behind the center of gravity symmetrically relative to the vertical plane of symmetry of the carrier aircraft. When synthesizing the laws for controlling the separation process, we will consider the longitudinal motion of the USR and CA. We will conventionally assume that we have one front support and one rear support. Let us assume that the USR is installed on the carrier aircraft in such a way that the axes of the associated coordinate systems USR and CA are parallel.

Figure 1 [21] shows simplified diagram of the USR connection to the carrier aircraft. The mechanism consists of a front (bow) rack and a rear (main) rack with a guide bar (strut). The struts are connected to the USR using ball joints and are rigidly attached to the carrier aircraft. For the stage of the joint flight as part of the ASS and the stage of separation of the USR and CA, we will consider the loads acting in a plane parallel to the vertical plane of symmetry of the aircraft. The expressions for the forces and moments will be considered in a connected coordinate system with the origin at the center of gravity of the booster unit (Fig. 2) [21]. Until the moment of separation (breaking of ties), the USR engines do not work. The figures 1 and 2 below are borrowed from the work [21].

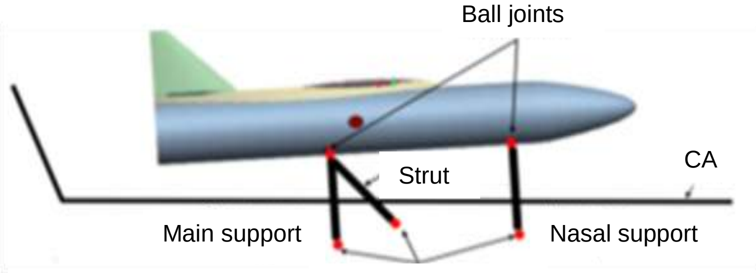

Figure 1. The scheme of fastening the USR to the CA.

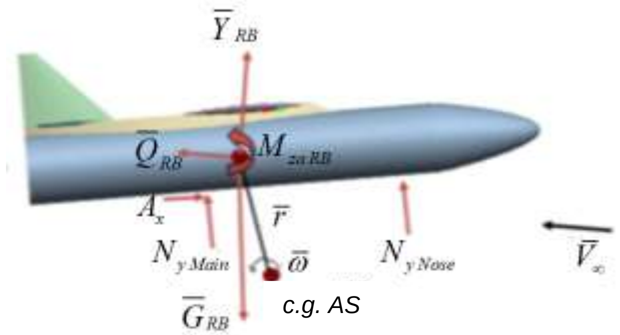

Figure 2. Diagram of forces and moments
acting on USR in free flight, and reaction forces from CA.

We assume that the front strut only accepts normal compressive or tensile loads, while the aft strut absorbs normal and axial loads due to the longitudinal brace. The proposed fastening design is a statically determinate system. Considering the acceleration and aerodynamic load on the aircraft, the normal and axial forces acting on the front and rear landing gear can be determined We assume that the front strut only accepts normal compressive or tensile loads, while the aft strut absorbs normal and axial loads due to the longitudinal brace. The proposed fastening design is a statically determinate system. Taking into account the acceleration and aerodynamic load on the aircraft, it is possible to determine the normal and axial forces acting on the front and rear struts. We assume that the front strut only accepts normal compressive or tensile loads, while the aft strut absorbs normal and axial loads due to the longitudinal brace. The proposed fastening design is a statically determinate system. Considering the acceleration and aerodynamic load on the aircraft, the normal and axial forces acting on the front and rear landing gear can be determined.

In the process of performing various evolutions by the carrier aircraft (maneuvers of pitching, diving, climb, descent, etc.), the upper stage located on the upper surface of the carrier aircraft makes a complex movement. The absolute speed of movement of the USR ($\bar{V}_{RB}$) is the sum of the portable speed of the entire AS ($\bar{V}$), applied at the center of gravity, and the relative speed of rotation of the USR around the center of gravity of the entire system (AS). When determining the speed and acceleration of the USR center of mass, we will use the formulas to describe the complex motion from the course of theoretical mechanics [22]:

$$\bar{V}_{RB} = \bar{V} + \bar{\omega}_{RB} \times \bar{r} \tag{5}$$

where $\bar{\omega}_{RB}$ – vector of the angular velocity of rotation of the USR around the center of mass of the ASS; $\bar{r}$ – radius-vector connecting c. g. AS and c. g. USR.

We determine the time derivative of the velocity of the center of mass of the USR and write down the equation of the dynamics of the translational motion of the USR in vector form:

$$m_{RB}\bar{a}_{RB} = m_{RB}(\bar{a} - \bar{\omega}_{RB}{}^{2} r\bar{e}_{r}) = \bar{F}_{RB} \tag{6}$$

where m_{RB} – weight of USR; $\bar{a}_{RB}$ – linear acceleration of USR; $\bar{a}$ – linear acceleration of AS; $\bar{F}_{RB}$ – the main vector of forces acting on the USR. The main vector of forces can be represented as follows:

$$\bar{F}_{RB} = \bar{G}_{RB} + \bar{R}_{RB} + \bar{P}_{RB} + \bar{N}_{RB} \tag{7}$$

where $\bar{G}_{RB}$ – gravity vector USR, $\bar{R}_{RB}$ – vector of the resultant aerodynamic force of the USR, $\bar{P}_{RB}$ – thrust vector USR, $\bar{N}_{RB}$ – vector of forces in the nodes of attachment of the upper stage to the carrier aircraft.

Figure 2 shows a diagram of the forces and moments acting on the USR in free flight; as well as the reaction forces acting on the USR from the side of the CA through the support brace system during a joint flight as part of the AS. For the rotation speed considered here, the induced speed is small and can be neglected. Then the resulting aerodynamic forces applied in c. g. of the upper stage, are determined for the speed of the undisturbed flow.

Let us determine the sum of the moments acting on the USR, relative to the main (rear) attachment point of the USR to the CA:

$$\sum M_{RB\_Main} = M_{G\_Main} + M_{a\_Main} + M_{Nn\_Main} \tag{8}$$

where M_{G_Main} – moment from gravity USR, M_{Nn_Main} – moment from the reaction force in the nasal attachment point. The aerodynamic moment M_{a_Main} acting relative to the center of gravity of the USR is brought to the attachment point of the main (rear) strut.

The time derivative of the velocity of motion of the center of mass of the USR $\bar{a}_{RB}$ is known at a given moment (at a given point). Aerodynamic forces can be determined from the results of scale models of blowing in wind tunnels, depending on the angle of attack and Mach number, or calculated using numerical aerodynamics methods [21]. Let's project the vector equation (6) on the axis O_1X_{RB} and O_1Y_{RB} the associated coordinate system. Its beginning coincides with the center of gravity of the upper stage, and the axes are located in the vertical plane of symmetry of the USR. Let us equate to zero the equation of moments (8), we obtain a system of 3 equations. This system is solved with respect to the following unknowns: two normal forces - in the bow node N_{yNose} and in the main node N_{yMain}, and the longitudinal force in the strut of the main node A_x. When both normal forces work in tension, the separation condition is reached.

The projections of the main vector of forces on the axis of the associated coordinate system are:

$$\begin{aligned} F_{xRB} &= G_{xRB} - X_{RB} + P_{xRB} + A_x; \\ F_{yRB} &= G_{yRB} + Y_{RB} + P_{yRB} + N_{yMain} + N_{yNose}, \end{aligned} \quad (9)$$

where X_{RB}, Y_{RB} – drag force and lifting force of the upper stage;

P_{xRB}, P_{yRB} – traction force projection USR;

G_{xRB}, G_{yRB} – gravity projection USR.

After a series of transformations, we obtain the projection of the forces in the attachment points:

$$\begin{aligned} N_{yNose} &= \frac{1}{r_{x\_Main\_Nose}}(-G_{xRB}r_{1yRB} + G_{yRB}r_{1xRB} + X_{RB}r_{1yRB} + Y_{RB}r_{1xRB}); \\ N_{yMain} &= (-V_x\omega_z + \omega_z^2 r_y + \frac{-mg\cos\vartheta + Y + P\sin\varphi_p}{m} - \frac{G_{yRB} + Y_{RB}}{m_{RB}})\frac{m_{RB}m}{m_{RB}+m} - N_{yNose}; \\ A_x &= (V_y\omega_z + \omega_z^2 r_x + \frac{-mg\sin\vartheta - X + P\cos(\varphi_p)}{m} - \frac{G_{xRB} - X_{RB}}{m_{RB}})\frac{m_{RB}m}{m_{RB}+m}, \end{aligned} \quad (10)$$

where $r_{x\_Main\_Nose}$ – the distance between the nose and main supports of the USR along the axis O_1X_{RB}; r_{1yRB}, r_{1xRB} – the shoulders of the gravity projections G_{xRB} and G_{yRB} relative to the main support, respectively; V_x, V_y – projections of the linear velocity vector of the center of mass of the carrier aircraft on the axis of the associated coordinate system; ω_z – angular pitch velocity of the carrier aircraft; ϑ – carrier aircraft pitch angle; X – drag force of the carrier aircraft; Y – lift of the carrier aircraft; P – total thrust force of the carrier aircraft engines; φ_p - the angle of installation of the engines of the carrier aircraft; m – mass of the carrier aircraft; r_x and r_y coordinates of the radius vector $\bar{r}$.

Using the transition matrix from a bound coordinate system to a semi-bound one, we get:

– force projection in the nasal support

$$N_{yNose}^{псв} = N_{yNose}\cos\alpha; \qquad N_{xNose}^{псв} = N_{yNose}\sin\alpha; \quad (11)$$

– force projection in the main support

$$\begin{aligned} N_{yMain}^{псв} &= -A_x\sin\alpha + N_{yMain}\cos\alpha; \\ N_{xMain}^{псв} &= A_x\cos\alpha + N_{yMain}\sin\alpha. \end{aligned} \quad (12)$$

Let us determine the moment from the forces in the supports relative to the center of gravity of the CA in the associated coordinate system:

$$M_{zN} = N_{yNose}h_{xNose} + N_{yMain}h_{xMain} - A_x h_{yMain} \tag{13}$$

где $h_{xNose}, h_{xMain}, h_{yMain}$ – the shoulders of the forces in the nose and main supports relative to the center of gravity of the carrier aircraft in the associated coordinate system.

2.1.3 Mathematical model in state variables

Taking into account the expressions (2, 4, 10÷13), and also taking into account the influence of interference from two closely spaced aircraft, the system of equations (1) will take the form:

$$\begin{aligned}
&\dot{x}_1(t) = \frac{u_2}{m}cos(x_3) - gsin(x_5 - x_3) + \frac{(N_{yNose} + N_{yMain})\sin(x_3) + A_x\cos(x_3) - qS(c_{x(\alpha)} + c_x^{\delta_в}u_1 + k_{in1}\Delta c_{xin})}{m};\\
&\dot{x}_2(t) = x_1 sin(x_5 - x_3);\\
&\dot{x}_3(t) = x_4 - \frac{u_2 sinx_3}{mx_1} + \frac{gcos(x_5 - x_3)}{x_1} + \frac{(N_{yNose} + N_{yMain})\cos(x_3) - A_x\sin x_3 - qS(c_{y(\alpha)} + c_y^{\delta_в}u_1 + k_{in2}\Delta c_{yin})}{mx_1};\\
&\dot{x}_4(t) = \frac{qSb_a}{I_z}\left[m_z(\alpha) + m_z^{\bar{\omega}_z}\frac{b_a x_4}{x_1} + m_z^{\delta_в}u_1 + k_{in3}\Delta m_{zin}\right] + \frac{1}{I_z}(N_{yNose}h_{xNose} + N_{yMain}h_{xMain} - A_x h_{yMain});\\
&\dot{x}_5(t) = x_4;\\
&\dot{x}_6(t) = x_1\cos(x_5 - x_3);\\
&A_x = (V_y x_4 + x_4{}^2 r_x + \frac{-mg\sin(x_5) - qS(c_{x(\alpha)} + c_x^{\delta_в}u_1 + k_{in1}\Delta c_{xin}) + u_2}{m} - \frac{G_{xRB} - X_{RB}}{m_{RB}})\frac{m_{RB}m}{m_{RB} + m};\\
&N_{yNose} = \frac{1}{r_{x_Main_Nose}}(-G_{xRB}r_{1yRB} + G_{yRB}r_{1xRB} + X_{RB}r_{1yRB} + Y_{RB}r_{1xRB});\\
&N_{yMain} = (-V_x x_4 + x_4{}^2 r_y + \frac{-mg\cos(x_5) + qS(c_{y(\alpha)} + c_y^{\delta_в}u_1 + k_{in2}\Delta c_{yin})}{m} - \frac{G_{yRB} + Y_{RB}}{m_{RB}})\frac{m_{RB}m}{m_{RB} + m} - N_{yNose}.
\end{aligned} \tag{14}$$

where $x_1 = V$, $x_2 = H$, $x_3 = \alpha$, $x_4 = \omega_z$, $x_5 = \vartheta$, $x_6 = x$ – state variables. Control actions: $u_1 = \delta_в$ – angle of deflection of the elevator of the carrier aircraft; $u_2 = P$– total thrust of the carrier aircraft.

System (1) is supplemented with algebraic equations of normal forces - in the nasal node N_{yNose} and in the main node N_{yMain}; as well as the longitudinal force in the strut of the main node A_x.

For the synthesis of control algorithms, the system of equations (14) is presented in state variables. Aerodynamic forces X and Y are preliminarily substituted.

2.2 Synthesis of control algorithms

The control task is to lift the aerospace system to a given altitude H^* (at which the USR will separate from the carrier aircraft), as well as to move the ASS at a given speed V^* at this altitude, that is, to create such starting conditions for the upper stage so that after completion of the separation maneuver with a carrier aircraft, he could make an autonomous flight with a climb.

Let us find in analytical form the control vector $u = [\delta_в(x_i), P(x_i)]$, depending on the state variables of the system (14), which ensures the fulfillment of the given technological invariants

$$V = V^*; \quad H = H^*. \tag{15}$$

The synthesis uses the standard ADAR procedure. For system (14), we introduce the following invariant manifolds:

$$\psi_1 = x_1 - x_1^* = 0; \qquad \psi_2 = x_4 - \varphi_1 = 0, \tag{16}$$

where x_1^* is the desired value of the variable corresponding to the set control goal (15); $x_1^* = V^*$; φ_1 - internal management.

Manifolds (16) must satisfy the solution of the system of functional equations [83]

$$T_1 \cdot \dot{\psi}_1 + \psi_1 = 0; \quad T_2 \cdot \dot{\psi}_2 + \psi_2 = 0, \tag{17}$$

where: T_1, T_2 – time constants affecting the quality of dynamic processes in the closed system "object of control - autopilot".

Asymptotic stability in the large of system (17) with respect to manifolds $\psi_1 = 0,\ \psi_2 = 0$ is ensured at $T_1 > 0, T_2 > 0$. As a result of the dynamic “contraction” of the phase space at the intersection of invariant manifolds $\psi_1 = 0,\ \psi_2 = 0$, the decomposed system will take the following form:

$$\dot{x}_2(t) = x_1^* \sin(x_5 - x_3); \quad \dot{x}_5(t) = \varphi_1. \tag{18}$$

For system (18), we introduce an invariant manifold ψ_3:

$$\psi_3 = x_1^* \sin(x_5 - x_3) + x_2 - x_2^* = 0, \tag{19}$$

where x_2^* is the desired value of the variable corresponding to the set control goal (15); $x_2^* = H^*$.

The joint analytical solution of equations (18), (19) and the functional equation $T_3 \cdot \dot{\psi}_3 + \psi_3 = 0$, allows you to find an expression for "internal" control φ_1, in the form of a function of state variables x_2, x_3, x_5, time constant T_3 and desired parameter values : x_1^*, x_2^*

$$\varphi_1 = -(1 + \frac{1}{T_3}) tg(x_5 - x_3) - \frac{x_2 - x_2^*}{T_3 x_1^* \cos(x_5 - x_3)} \tag{20}$$

According to the procedure of the ADAR method, from the joint solution of (16), (20), the system of functional equations (17) and equations of the model (14), we obtain expressions for the control actions: the deflection angle of the elevator $\delta_в$ and the thrust of the engines P. These expressions are external controls and are functions that depend on the system state variables

$$u_1, u_2 = f(x_1, x_2, x_3, x_4, x_5, x_6). \tag{21}$$

After substituting the expressions for the control actions into the model of the control object (14), we obtain a closed nonlinear motion control system of the aerospace complex. By setting the parameters of the controller and choosing the invariants, we obtain a system that depends only on the state variables.

Below are the results of numerical studies of the dynamic properties of the resulting closed-loop system.

2.3 Simulation

For the numerical solution of a closed nonlinear system, we will use the Runge-Kutta method of the 4th order, the Maple software package. Figures 3–8 show the simulation results, namely: the dependence of phase variables on time (Fig. 3, 4, 7); change of control actions with respect to integration time (Fig. 5-6). Figures 3-4 show that the aerospace complex achieves the desired speed of 800 km / h and a flight altitude of 10,000 m; the pitch angular velocity (Fig. 7) decays, and the invariant manifolds tend to zero (Fig. 8).

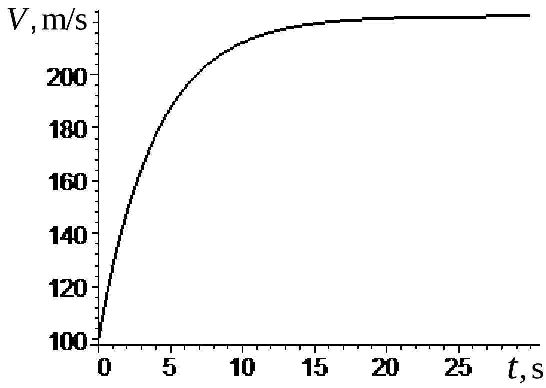

Figure 3 – Flight speed.

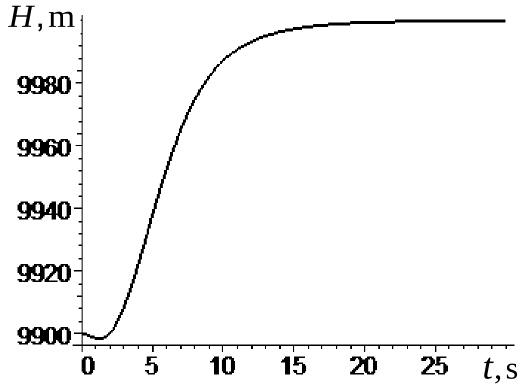

Figure 4 – Flight altitude.

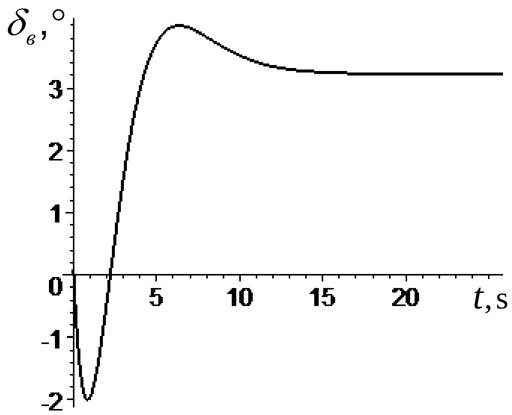

Figure 5 – Control u_1.

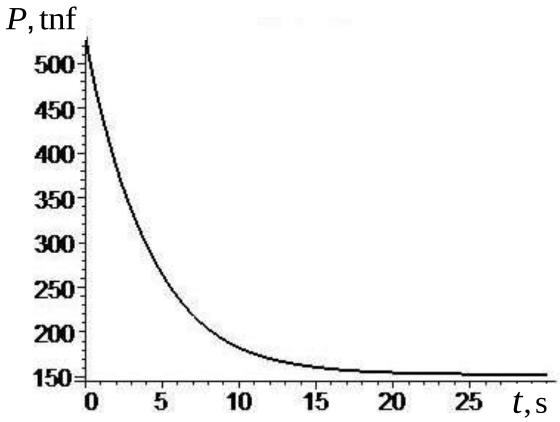

Figure 6 – Control u_2.

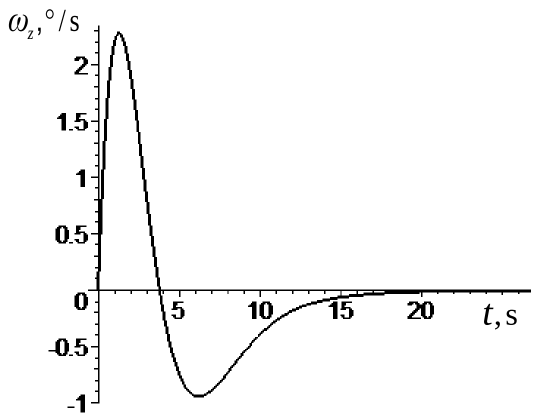

Figure 7 – Angular Pitch Velocity.

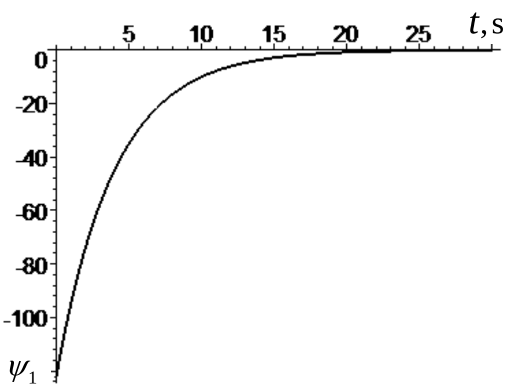

Figure 8 – Invariant manifold.

The simulation results show that the motion of the closed-loop system is asymptotically stable in the entire region of the phase space for various combinations of the initial values of the state coordinates. The exception is the points at which the considered mathematical model of the object is not defined (at an angle of attack and an angle of inclination of the trajectory equal to 90 degrees).

3. Synthesis of control algorithms for the separation of USR and CA with simultaneous breaking of bonds

3.1 Aircraft separation technique

Let us consider the process of separating the upper stage from the CA by creating angular pitch velocities of the opposite sign.

Before the start of separation, the elevator of the USR is deflected with its tail up "for pitching", while the elevator of the carrier aircraft is deflected with its tail down "for a dive". At the same time, all three locks of the mechanism for attaching the upper stage to the carrier aircraft are opened, and mechanical bonds are broken. The separated USR under the influence of the elevator rotates in the direction of "pitch-up". Its angle of attack increases and a positive increase in lift appears. At the same time, the carrier aircraft turns in the dive direction. Its angle of attack and lift are reduced and the carrier aircraft moves downward with a decrease in the angle of inclination of the trajectory (fig. 9).

When the USR turns "to pitch up", and the CA "to dive", the tail section of the USR fuselage is lowered and the tail section of the CA is raised. Therefore, at the initial moment of rotation, it is necessary to strictly control the gap between the aircraft in order to avoid their collision during the separation process.

In the passive phase of the flight, the USR engines have not yet been turned on, and it moves with a lag in relation to the carrier aircraft. The jet engines of the upper stage are switched on a few seconds after reaching a safe distance between the USR and the CA.

The active phase of the USR flight with respect to the CA begins. The upper stage begins to move forward in relation to the carrier aircraft. In this case, it is necessary to exclude the entry of the carrier aircraft into the jet stream of gases from the engines of the upper stage [23]. These restrictions on the flight trajectory of the upper stage in the passive and active sections should be taken into account when setting the problem of synthesizing the autopilot laws of motion control of both aircraft in the process of their separation.

Figure 9 – Aircraft separation scheme.

3.2 Mathematical model

To synthesize the laws of separation control with the simultaneous breaking of all bonds, we will use the mathematical model (14), supplementing it with a similar model for the upper stage in state variables:

$$\begin{aligned}
&\dot{x}_7(t)=\frac{u_4}{m_{RB}}cos(x_9)-gsin(x_{11}-x_9)+\\
&+\frac{(-N_{yNose}-N_{yMain})\sin(x_9)+A_x\cos(x_9)-q_{RB}S_{RB}(c_{x(\alpha)RB}+c_{x\,RB}^{\delta_{в RB}}u_3+k_{in1RB}\Delta c_{xin\,RB}+\Delta c_{x\,BKC})}{m_{RB}};\\
&\dot{x}_8(t)=x_7 sin(x_{11}-x_9);\\
&\dot{x}_9(t)=x_{10}-\frac{u_4 sinx_9}{m_{RB}x_7}+g\frac{cos(x_{11}-x_9)}{x_7}+\\
&+\frac{(-N_{yNose}-N_{yMain})\cos(x_9)-A_x\sin(x_9)-q_{RB}S_{RB}(c_{y(\alpha)RB}+c_{y\,RB}^{\delta_{в RB}}u_3+k_{in2RB}\Delta c_{yin\,RB}+\Delta c_{y\,BKC})}{m_{RB}x_7};\\
&\dot{x}_{10}(t)=\frac{q_{RB}S_{RB}b_{a\,RB}}{I_{z\,RB}}(m_{z\,RB}(\alpha_{RB})+m_{zRB}^{\bar{\omega}_{z\,RB}}\frac{b_{a\,RB}x_{10}}{x_7}+m_{z\,RB}^{\delta_{в RB}}u_3+k_{in3RB}\Delta m_{zinRB})+\\
&+\frac{1}{I_{z\,RB}}(-N_{yNose}h_{xNose}-N_{yMain}h_{xMain}-A_x h_{yMain});\\
&\dot{x}_{11}(t)=x_{10};\\
&\dot{x}_{12}(t)=x_7 cos(x_{11}-x_9).
\end{aligned} \tag{22}$$

where the state variables $x_7=V_{RB}$, $x_8=H_{RB}$, $x_9=\alpha_{RB}$, $x_{10}=\omega_{zRB}$, $x_{11}=\vartheta_{RB}$, $x_{12}=x_{RB}$ – speed, altitude, angle of attack, angular pitch rate, pitch angle, longitudinal displacement, respectively, of the upper stage. Control actions: $u_3=\delta_{вRB}$ – deflection angle of the elevator USR; $u_4=P_{RB}$– total thrust of the USR power plant.

Goal of management:

1) ensuring the movement of the CA along a downward trajectory immediately after the moment of separation with the achievement of the desired speed and altitude;

2) ensuring the autonomous movement of the USR after breaking the mechanical bonds along the ascending trajectory and achieving the desired altitude and flight speed:

$$V=V^*;\quad H=H^*;\quad V_{RB}=V_{RB}^*;\quad H_{RB}=H_{RB}^*. \tag{23}$$

Formulation of the problem. It is required to find in analytical form the control vector that ensures the reduction of the CA to altitude H^* with acceleration to speed V^*; as well as starting the USR engines at a safe distance from the CA, raising the USR to a given height H_{RB}^*, and achieving the desired speed V_{RB}^*.

3.3 Synthesis of control algorithms

The synthesis of control laws is similar to that given in Section 2.2.

According to the procedure of the ADAR method, we introduce invariant manifolds

$$\begin{aligned}
&\psi_1=x_1-x_1^*=0;\quad \psi_3=x_7-x_7^*=0;\\
&\psi_2=x_4-\varphi_1=0;\quad \psi_4=x_{10}-\varphi_2=0,
\end{aligned} \tag{24}$$

where $x_1^*=V^*$; $x_7=V_{RB}^*$; φ_1, φ_2 – internal controls.

Manifolds (24) must satisfy the solution of the system of functional equations:

$$\begin{aligned}
&T_1\cdot\dot{\psi}_1+\psi_1=0;\quad T_3\cdot\dot{\psi}_3+\psi_3=0;\\
&T_2\cdot\dot{\psi}_2+\psi_2=0;\quad T_4\cdot\dot{\psi}_4+\psi_4=0,
\end{aligned} \tag{25}$$

where: T_1, T_2, T_3, T_4. – time constants.

The decomposed system will take the form:

$$\begin{aligned} &\dot{x}_2(t) = x_1^* \sin(x_5 - x_3); \quad \dot{x}_5(t) = \varphi_1; \\ &\dot{x}_8(t) = x_7^* \sin(x_{11} - x_9); \quad \dot{x}_{11}(t) = \varphi_2. \end{aligned} \tag{26}$$

For system (26), we introduce the invariant manifolds ψ_5, ψ_6:

$$\begin{aligned} &\psi_5 = x_1^* \sin(x_5 - x_3) + x_2 - x_2^* = 0; \\ &\psi_6 = x_7^* \sin(x_{11} - x_9) + x_8 - x_8^* = 0, \end{aligned} \tag{27}$$

where x_2^*, x_8^* – the desired values of the variables corresponding to the set control objectives (23), $x_2^* = H^*$, $x_8^* = H_{RB}^*$. Having solved analytically jointly equations (26), (27) and functional equations

$$T_5 \cdot \dot{\psi}_5 + \psi_5 = 0; \quad T_6 \cdot \dot{\psi}_6 + \psi_6 = 0, \tag{28}$$

find expressions for "internal" controls φ_1, φ_2. Internal control φ_1 depends on phase variables x_2, x_3, x_5, time constant T_5 and technological invariants ; x_1^*, x_2^*; φ_2 is a function of state variables x_8, x_9, x_{11}, time constant T_6 and desired parameter values x_7^*, x_8^*.

$$\varphi_1 = -(1 + \frac{1}{T_5}) tg(x_5 - x_3) - \frac{x_2 - x_2^*}{T_5 x_1^* \cos(x_5 - x_3)}; \quad \varphi_2 = -(1 + \frac{1}{T_6}) tg(x_{11} - x_9) - \frac{x_8 - x_8^*}{T_6 x_7^* \cos(x_{11} - x_9)} \tag{29}$$

Further, having solved together (24), (29), the system of functional equations (25) and the system of equations of the model (22), we obtain expressions for the deflection angle of the elevator $\delta_в$ and the thrust of the engines of the carrier aircraft P; as well as the deflection angle of the elevator $\delta_{в RB}$ and the thrust of the upper stage engines P_{RB}. These control actions are external controls and are functions that depend on the system state variables:

$$\begin{aligned} &u_1, u_2 = f(x_1, x_2, x_3, x_4, x_5, x_6); \\ &u_3, u_4 = f(x_7, x_8, x_9, x_{10}, x_{11}, x_{12}). \end{aligned} \tag{30}$$

3.4 Simulation

3.4.1 Initial data for modeling

Initial conditions: V (0) = V_{RB} (0) = 800 km/h (222,2 m/s) – the flight speed of the carrier aircraft and the upper stage as part of the AS; H (0) = H_{RB} (0) = 10000 m – flight altitude of the carrier aircraft and the upper stage as part of the AS; α (0) = α_{RB} (0) = 2,4 deg; ω_z (0) = ω_{zRB} (0) = 0 deg/s; ϑ (0) = ϑ_{RB} (0) = 2,4 deg; x (0) = x_{RB} (0) = 270000 m.

Invariants:

H^* = 9950 m – the height to which the CA decreases after the moment of separation;

V^* = 230 m/s – the speed to which the carrier aircraft is accelerated;

H_{RB}^* = 10020 m – the height to which the USR rises after the separation of the aircrafts;

V_{RB}^* = 215 m/s – the desired speed to which the acceleration unit is decelerated.

Controller parameters: T_1 = 2 s; T_2 = T_5 = 2,5 s, T_3 = 2 s; T_4 = T_6 = 2,5 s.

For the numerical solution of a closed nonlinear system of differential equations (22), (30), the Maple software package and Gear's method were used.

3.4.2 Transients and analysis of results

Figures 10–19 show the results of modeling the dynamics of the motion of the resulting closed-loop system "carrier aircraft - upper stage - autopilot control laws". Figure 10 shows the change in the height of the carrier aircraft and the upper stage. The separation of aircraft occurs at the 10th second after the start of the simulation of the dynamics of the movement of the AS. After separation, the carrier aircraft descends from an altitude of 10000 meters to the desired altitude of 9950 meters and then levels off. The upper stage moves with an increase in flight altitude until the specified invariant H^*_{RB} = 10020 m is reached.

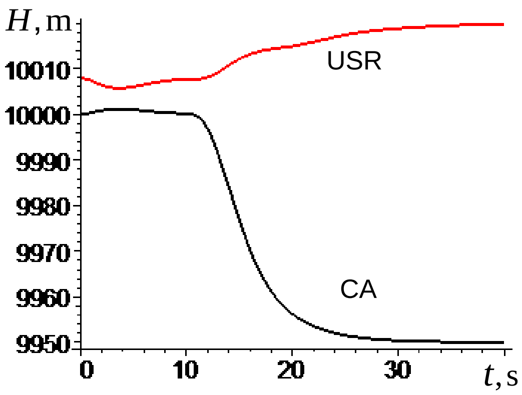

Figure 10 – Flight altitude CA and USR.

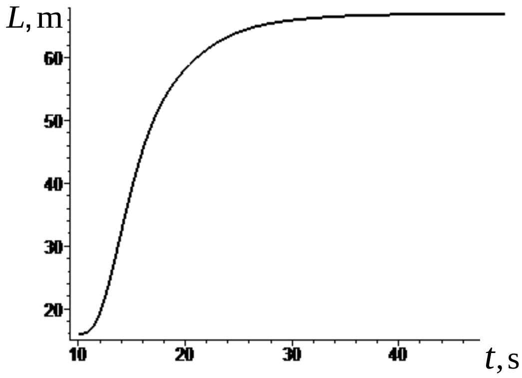

Figure 11 – Distance between CA and USR

Figure 11 shows the vertical distance between the carrier aircraft and the upper stage. The interference effect between the two aircraft disappears approximately at the 7th second after the moment of separation (17th second on the graph), when the vertical distance between the centers of gravity of the aircrafts exceeds 60 meters.

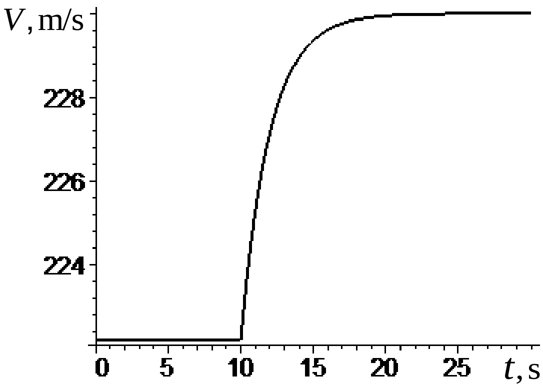

Figure 12 – Flight speed CA.

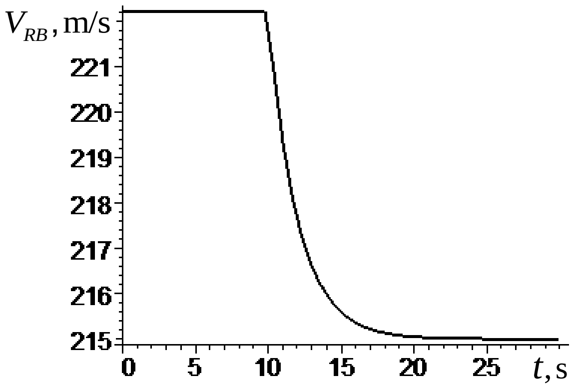

Figure 13 – Flight speed USR.

Figures 12 and 13 show the time variation of the flight speed of the carrier aircraft and the upper stage. Graphs show that from the 1st to the 10th second of the simulation, the carrier aircraft and the upper stage move as part of the aerospace system. The AS is balanced in steady level flight without roll and slip at a speed of Mach 0.7, flight altitude is 10000 meters. Simulation shows that at the 10th second all mechanical connections are broken, and upper stage separates from the carrier aircraft. Carrier aircraft descends (Fig. 10) and accelerates to a speed of V^* = 230 m/s (Fig. 12). In this case, the upper stage moves with an increase in flight altitude (Fig. 10) and decelerates to a speed of V^*_{RB} = 215 m/s (Fig. 13).

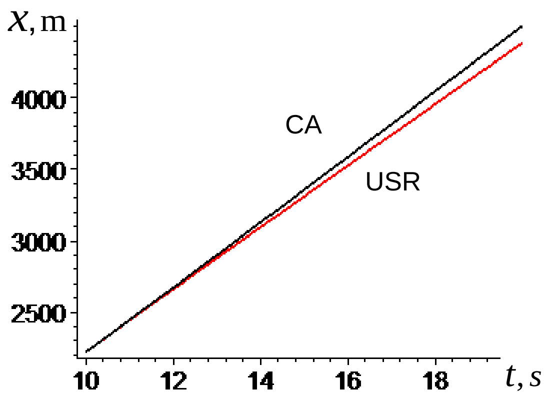

Figure 14 – Path covered by CA and USR.

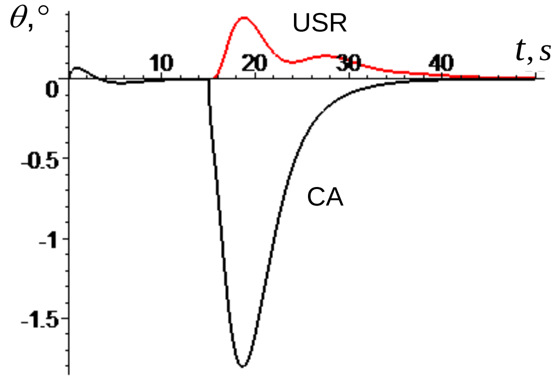

Figure 15 – Trajectory slope CA and USR.

Figure 14 shows the path traveled by CA and USR. The upper stage moves lagging behind the carrier aircraft. The probability of hitting the carrier aircraft in the high-temperature jet stream from the rocket engines of the upper stage is reduced.

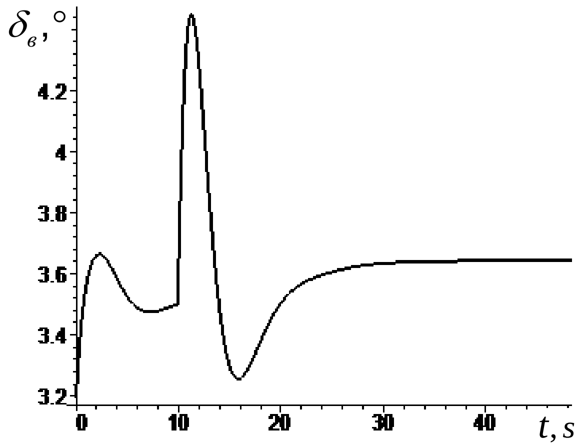

Figure 16 – Control u_1.

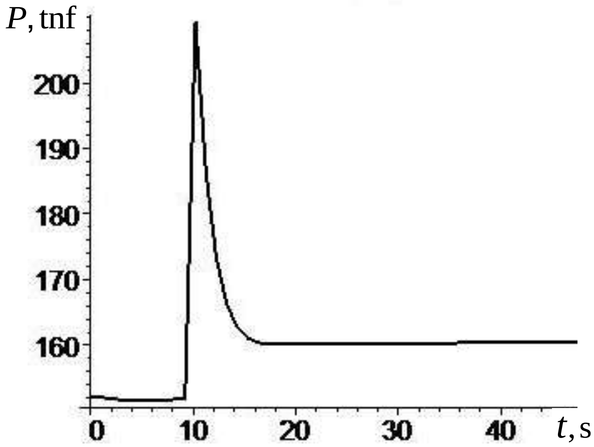

Figure 17 – Control u_2.

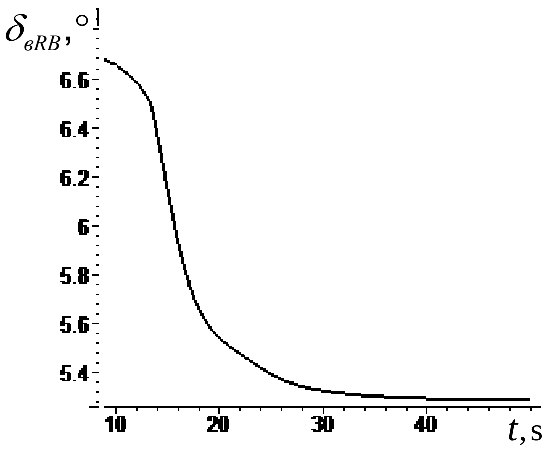

Figure 18 – Control u_3.

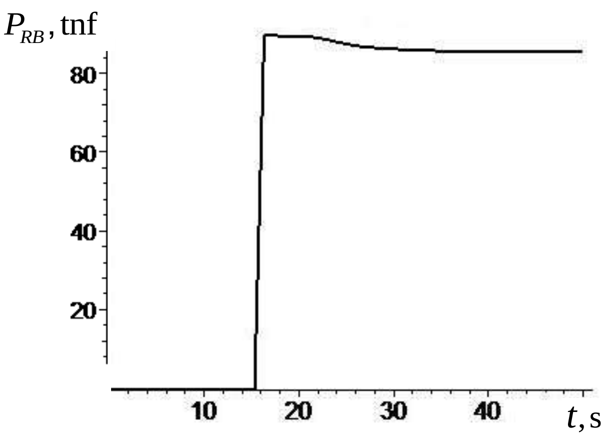

Figure 19 – Control u_4.

The change in the control actions with respect to the integration time for the carrier aircraft is shown in Fig. 16-17. Control laws for the upper stage: the deflection angle of the elevator and the thrust of the engines depending on time are presented in Fig. 18-19.

Immediately before the separation, the deflection angle of the upper stage's elevator decreases, turning the USR “to pitch up” (Fig. 18). The engines of the upper stage are switched on 6 seconds after the separation of the USR from the CA (Fig. 19)

4. Conclusion

An adequate mathematical model of the longitudinal motion of the aerospace system, as well as a mathematical model of forces in the communication nodes between the carrier aircraft and the upper stage, has been developed.

Based on the provisions of the synergetic control theory and the ADAR method, the following were developed:

– AS control algorithm when ascending to a given altitude at a given speed, providing the required starting conditions for the upper stage (altitude 10 km, speed 800 km / h);

– an algorithm for controlling the air launch of the upper stage from the carrier aircraft while simultaneously breaking the connections between them. This guarantees shockless separation of the USR and CA and their subsequent movement along independent trajectories with stabilization of speed and altitude for each aircraft.

The results of the study and computer modeling show that the synthesized control laws provide asymptotic stability of closed systems in the entire permissible range of phase coordinates and the achievement of the set control goals at all considered stages of launching the aerospace system.

5. Contact Author Email Address

Mailto: olgadmk@yandex.ru

6. Copyright Statement

References

[1] Decker I, Wilhite A. Technology and methology of separating two similar size aerospace vehicles within the atmosphere. *AIAA Paper*, No. 75 – 29, 1975

[2] Moelyadi M, Breitsamter C, Laschka B. Steady and unsteady calculations on full configuration of two-stage space transportation system during separation. *24th International Congress of the Aeronautical Sciences, ICAS2004*, 2004

[3] Decker J and Gera J. An exploratory study of parallel stage separation of reusable launch vehicles. *NASA TN D-4765*, 1968

[4] Decker K. Aerodynamics of a two-stage space transport system on re-entry and during separation. *Dissertation*, Technical University of Munich, 2003

[5] Bernot P. Abort separation study of a shuttle orbiter and external tank at hypersonic speed. *NASA.TM X-3212*, 1975

[6] Rochholz H, Huber T, Matyas F. Unsteady airloads during separation of an idealized two-stage hypersonic vechicle. *Zeitchrift fur Flugwissenschaften und Weltraumforchung*, Vol. 19, Is. 1, pp 2-9, 1995

[7] Demeshkina V, Ilyin V, Leutin A. Some features of the process of separation of aircraft near the moment of breaking the bonds. Part I. *TsAGI Science Journal*, Vol. 11, No. 4, 1980

[8] Leutin A. On the determination of the system of reaction forces in the hinged attachment points of aircraft during their separation. *TsAGI Science Journal*, Vol. 12, No. 4, 1981

[9] Ilyin V. Friction force and moment of friction forces in the hinged attachment points when turning two aircraft relative to these nodes. Part I and II. *TsAGI Science Journal*, Vol. 16, No. 3, 1985 and Vol. 17, No. 1, 1986

[10] Ovchinnikov V, Sadchikov V. Determination of linear and angular accelerations of a non-free system of two flying ones. *TsAGI Science Journal*, Vol. 18, No. 5, 1987

[11] Letov A. Analytical design of regulators, I, II, III. *Automation and telemechanics*, No. 4, 5, 6, 1960.

[12] Krasovskiy A., *Guide book for automatic control theory*. M. Nauka, 1987

[13] Bukov V. *Adaptive forecasting flight control systems*. M. Nauka, 1987

[14] Miroshnik I, Nikiforov V, Fradkov A. *Nonlinear and adaptive control of complex dynamic systems*. SPb. Nauka, 2000

[15] Aizenberg Ya, Sukhorebryi V. *Design of systems for stabilization of carriers of space vehicles*. M. Mashinostroyeniye, 1986

[16] Kolesnikov A. *Synergic control theory*. M. Energoatomizadt, 1994

[17] Kolesnikov A. Analytical design of nonlinear aggregated controllers for a given set of invariant manifolds. II. Vector control. *Izvestiya vuzov. Electromechanics*, No. 5, 1987

[18] Kolesnikov A, Kobzev V. *Flight dynamics and control: synergic approach.* Taganrog. TTI YuFU, 2009

[19] Byushgens G., Studnev R. *Aeroplane dynamics: spatial motion*. M: Mashinostroenie, 1983

[20] GOST 20058-80. *Dynamics of aircraft in the atmosphere: Terms, definitions and symbols.* M. Izd-vo standartov, 1981.

[21] Mehta U, Bowles J, Pandya S, Melton J, Huynh L, Kless J, Hawke V, Conceptual stage separation from widebody subsonic carrier aircraft for space access. *The Aeronautical Journal*, Vol. 118, No. 1209, pp 1279-1303, 2014

[22] Trukhan N. *Kinematics. Methodical instructions for solving problems for the course: Theoretical mechanics.* M. MPTU, 1991

[23] Kuzyakin Yu. Air launch of carrier rockets from the upper part of the aircraft fuselage. *Adaptive systems and automatic control: multidisciplinary science and technology collection*, No. 13 (33), pp 45-54, 2008